Aust. J. Phys., 1983, **36**, 185–96

Elastic and Inelastic Scattering of Gamma Rays from V_3Si

S. S. Ti,[A,B] *T. R. Finlayson,*[A] *T. F. Smith,*[A]
J. D. Cashion[A] *and P. E. Clark*[A,C]

[A] Department of Physics, Monash University, Clayton, Vic. 3168.
[B] Present address: Wellington High School, Mulgrave, Vic. 3170.
[C] Present address: Department of Applied Physics,
Capricornia Institute of Advanced Education, Rockhampton, Qld 4700.

Abstract

The elastic and inelastic components of γ-ray scattering from a non-transforming V_3Si single crystal have been measured using a ^{57}Co Mössbauer source and resonant absorber. The system places an upper limit of $\pm 4 \times 10^{-8}$ eV on the possible energy transfer which distinguishes inelastic from elastic scattering. The scattering at the (440) Bragg reflection with $q = 0$ and $q \sim 0{\cdot}1$ Å^{-1} has been measured as a function of temperature for two orthogonal orientations of the crystal. Anomalous changes in the elastic and inelastic intensities have been observed. It is suggested that these changes are associated respectively with central mode and soft mode aspects of the dynamics of the vanadium atoms.

1. Introduction

The A15 structure compounds V_3Si and Nb_3Sn have been studied extensively on account of their high superconducting transition temperatures (T_c is 17 K for V_3Si and 18 K for Nb_3Sn) and the phase transitions at $T_m > T_c$, which are known to involve lattice vibrational instabilities (Testardi 1973). For both compounds the [110] transverse acoustic (TA) phonons with [$1\bar{1}0$] polarization have been found to show a marked softening on cooling from room temperature, resulting in a transition in some samples from the cubic to a tetragonal structure at T_m. For V_3Si and Nb_3Sn, T_m is 21 K and 45 K respectively.

Neutron diffraction measurements on Nb_3Sn (Shirane and Axe 1971) have revealed the development of reflections in the tetragonal phase below 45 K which are forbidden in the cubic phase and have been identified with static displacements of the niobium atoms. In subsequent inelastic neutron scattering studies (Axe and Shirane 1973) a central peak was found to appear and grow in intensity as $T \to T_m$ from above. For V_3Si, although the softening of the [110] TA mode has been demonstrated by neutron scattering (Shirane *et al.* 1971), the large incoherent scattering cross section for the vanadium atoms prevents any detailed study of the dynamic scattering. The possible existence of any softening of the optic modes could not be determined.

Kodess (1974), in X-ray studies of specific Bragg reflections from V_3Si, reported an anomalous decrease in intensity for the (440) peak as the temperature was lowered. This involves structure factor contributions from both vanadium and silicon atoms, but only the normal increase in intensity was seen for a (320) peak involving only vanadium atom contributions. These data were interpreted by Kodess as evidence

0004-9506/83/020185$02.00

for an increase in the vibrational amplitude of the Si atoms, the sublattice of which ultimately distorts at the structural transition.

In direct contradiction to this, Staudenmann and Testardi (1979) have concluded from the analysis of the integrated intensities of over 1000 X-ray reflections from single crystal V_3Si that the motion of the vanadium atoms is highly anharmonic, so that they spend a longer time at the extremities of their travel than would be the case for harmonic motion. They found no unusual behaviour for the Si atoms.

To investigate further the low-temperature lattice dynamics of V_3Si, we have applied the non-resonant Mössbauer scattering technique to the study of the temperature dependence of the elastic and inelastic scattering from a V_3Si single crystal. In this paper we report the data for the (440) and (421) Bragg reflections, where the former involves both vanadium and silicon contributions to the structure factor but the latter only has vanadium contributions.

2. Experimental Details

Two specimens of V_3Si were spark cut from the same single crystal with faces parallel to the (110) and (421) planes. We shall refer to these as the (110) and (421) crystals respectively. Both samples had elliptical cross sections of approximately 9·5 by 8 mm and thicknesses of 6 and 1 mm respectively. This single crystal was the same one from which samples had been taken for superconductivity (Smith 1972) and specific heat (Viswanathan and Luo 1971; Viswanathan and Johnston 1976) measurements. The former set of these specific heat data indicated that the crystal does not undergo the cubic to tetragonal distortion on cooling while the latter suggested quite the reverse. However, elastic measurements made on the whole (110) crystal (J. A. Rayne, T. R. Finlayson and T. F. Smith, unpublished data) showed no evidence for this distortion.

The specimens were aligned by the Laue method to an accuracy of $\pm 2°$ at room temperature. In addition to these photographs, others were also taken for the (110) crystal at 9 and 18 K to determine whether there was any evidence for the cubic to tetragonal distortion. No spot splitting or streaking could be detected, reinforcing the earlier evidence that the crystal remains cubic. Quite distinct spot splitting has been observed for another crystal which is known to distort.

After the alignment, the specimen was mounted on the sample stage of a modified Oxford Instruments continuous flow cryostat model CF 100. Mössbauer scattering measurements were made using the experimental arrangements described previously (Ti *et al.* 1982). Briefly, the specimen was irradiated by a 100 mCi ^{57}Co*Rh* source of diameter 4·5 mm, and the scattered γ rays were detected by either a Si(Li) or a Ge(Li) detector. The signal-to-noise ratio was always better than 6 : 1 and up to 23 : 1. The absorber used was lithium ammonium fluoferrate, which was 95% enriched with $2\ \mathrm{mg\,cm^{-2}}$ of ^{57}Fe, and gave an energy resolution $\sim \pm 4 \times 10^{-8}$ eV. The experiment was performed in an 'on–off' mode (O'Connor 1972; Albanese and Ghezzi 1972) where the fraction of γ rays elastically scattered from the crystal is given by

$$f_e = R(\theta)/R(0). \tag{1}$$

The resonant fractions of the scattered and incident beams, $R(\theta)$ and $R(0)$ respectively, are determined from the background-corrected count rates for the scattered beam with the absorber removed, I_θ, with the absorber placed at rest between the sample and the detector, I_θ^a, and between the source and the sample, I_0^a, using the expressions

$$R(\theta) = (I_\theta - I_\theta^a)/I_\theta = f_s f_e (1-x), \tag{2}$$

$$R(0) = (I_\theta - I_0^a)/I_\theta = f_s (1-x), \tag{3}$$

where f_s is the recoilless fraction of the source and x the fraction of resonant γ rays absorbed by the absorber. Both I_θ^a and I_0^a are corrected for photoelectric absorption by the absorber ($\sim 15\%$) and for change in the measured intensities due to the radioactive decay of the source, prior to the evaluation of the elastic fraction f_e. The total scattered γ intensity I_θ is decomposed into elastic I_e and inelastic I_i components with

$$I_e = I_\theta f_e, \tag{4}$$

$$I_i = I_\theta (1-f_e). \tag{5}$$

With our present experimental arrangement, which does not allow for the re-positioning of the absorber in the incident and scattered beams with high precision, it was found that repeated room-temperature determinations of $R(0)$ (the resonant fraction of the incident beam) gave values which varied by as much as $\pm 10\%$. We attribute this to changes in the fractional transmission of the resonant radiation, as represented by the parameter x, arising from inherent inhomogeneities in the analysing black absorber and slight variations in the areas placed in the scattered and incident beams. To avoid this uncertainty when determining $R(\theta)$ as a function of temperature, a full set of measurements of I_θ^a was taken without disturbing the analyser, after which it was removed and a further full set of measurements of I_θ was made at the same temperatures. In this manner reliable relative values for f_e as a function of temperature could be obtained even though the uncertainty in the absolute values was of order $\pm 10\%$.

(*a*)

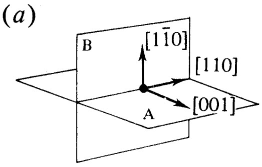

(*b*)

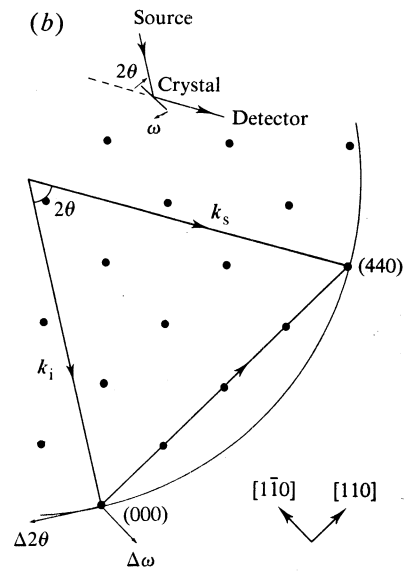

Fig. 1. (*a*) Geometry of scattering planes for settings A and B used for measurements about the (440) Bragg reflection. (*b*) Reciprocal space scattering geometry for setting B of the (110) crystal. The directions of the scans for independent rotations of the source $\Delta\omega$ and the sample $\Delta 2\theta$ with fixed detector are shown.

The background intensity was checked periodically during the course of the measurements by removing the 14·4 keV radiation with an aluminium filter and was found to be constant within experimental error.

Multiple measurements of the (440) Bragg reflection were carried out in different scanning modes in order to investigate the influence of various phonons on the inelastic scattering. Initially the crystal with the (110) face was set with its [001] direction on the face oriented horizontally so that [110] and [001] defined the scattering plane. This is denoted as setting A (see Fig. 1*a*) and it made $[1\bar{1}0]$ vertical and collinear with the axis of the cryostat, which was also the axis of rotation of the crystal. A second setting B was obtained by rotating the crystal through 90° about [110] so that $[1\bar{1}0]$ was in the scattering plane and [001] became collinear with the vertical rotation axis.

The scattering geometry in the present measurements differs from the conventional X-ray geometry in that it is the source instead of the detector that is rotated. However, for convenience we retain the conventional notation and consider both crystal and source rotations to be positive in a clockwise direction and denote these as ω and 2θ scans respectively. This is illustrated in Fig. 1*b* along with the corresponding scattering geometry in reciprocal space appropriate to setting B of the crystal. The initial directions for the scans in reciprocal space corresponding to the changes $\Delta 2\theta$ and $\Delta\omega$ are also indicated. Note that although the rotation of the crystal rotates the reciprocal lattice in a clockwise direction about the (440) reciprocal lattice point, the region of reciprocal space illuminated by the incident radiation moves in the opposite direction.

The Bragg peaks were scanned by three methods: rotating the source (2θ scan), rotating the crystal (ω scan) and rotating both the crystal and source such that $\Delta 2\theta = 2\Delta\omega$ ($\omega/2\theta$ scan).* These three rotations set different conditions on the allowed direction of $\boldsymbol{q}$, the phonon wave vector involved in inelastic scattering. In addition, the scanning conditions are also expected to influence the scattered intensities due to the spatial distribution of the Bragg reflection arising from the mosaic and possibly multifragment composition of the crystal, the extended nature and inhomogeneity of the source and the relatively poor collimation (Mathieson 1982).

Scans across the Bragg peak were made at fixed temperatures for the following conditions:

(1) A(2θ) giving $\boldsymbol{q}$ at an angle 31° to [110] (59° to [001]);

(2) A(ω) giving $\boldsymbol{q}$ parallel to [001];

(3) A($\omega/2\theta$) giving $\boldsymbol{q}$ parallel to [110];

(4) B(ω) giving $\boldsymbol{q}$ parallel to $[1\bar{1}0]$.

Runs at fixed angle and variable temperature were made under the conditions:

(5) A on the Bragg peak, from 293 to 5 K;

(6) A(2θ) with the source rotated 1° from the Bragg condition, from 293 to 5 K, $|\boldsymbol{q}| = 0{\cdot}13\ \text{Å}^{-1}$;

(7) B on the Bragg peak, from 40 to 5 K;

(8) B(ω) with the crystal rotated 0·5° from the Bragg condition, from 40 to 5 K, $|\boldsymbol{q}| = 0{\cdot}07\ \text{Å}^{-1}$.

* In terms of the conventional X-ray scattering geometry the present scans in reciprocal space have the following equivalences: $2\theta \equiv \omega/\theta$, $\omega/2\theta \equiv \omega/2\theta$ and $\omega \equiv \omega$.

Finally the (421) crystal was examined with a 2θ scan at fixed temperature and a temperature scan (27·5–11 K) while centred on the Bragg peak.

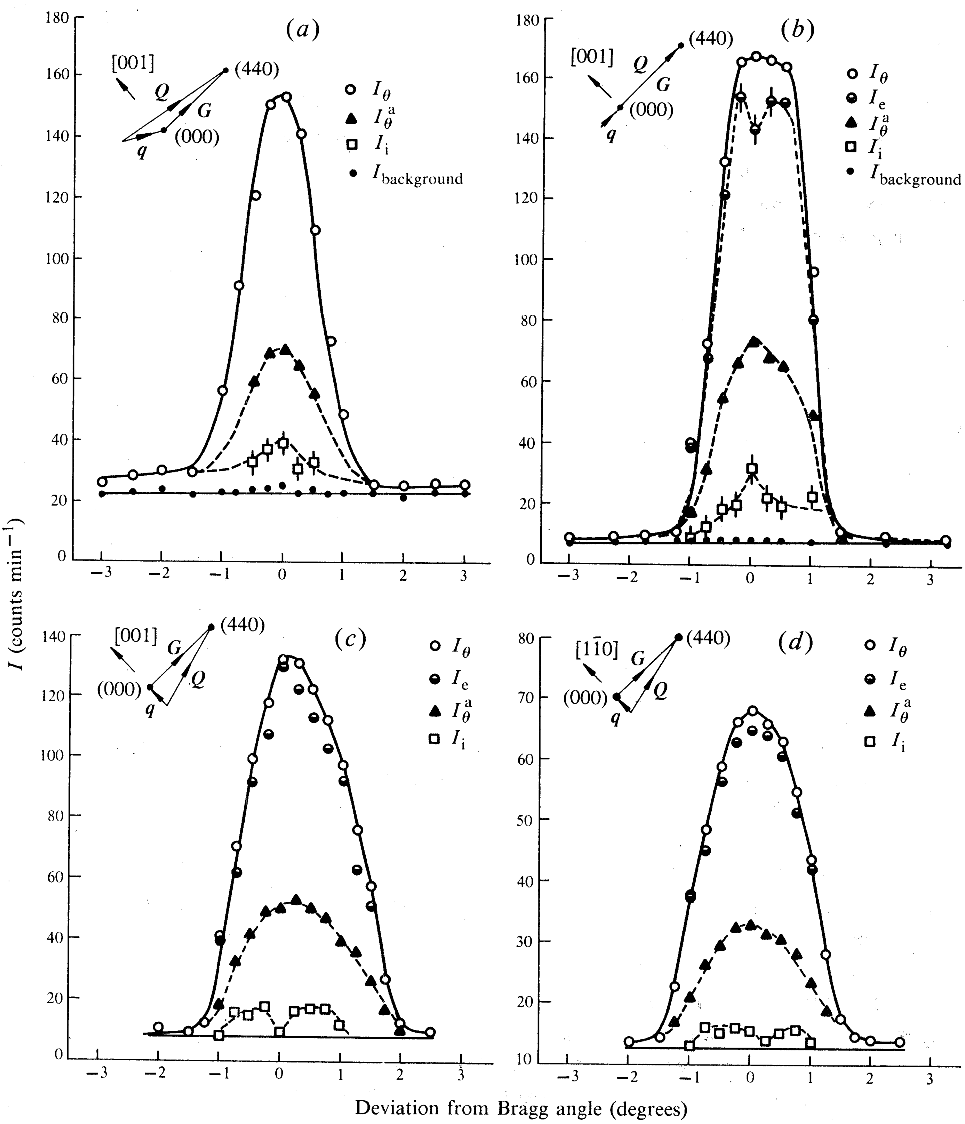

Fig. 2. Scans of the (440) Bragg reflection of V_3Si at (*a*) 293 K, scanned under condition A(2θ) with Ge(Li) detector; (*b*) 18 K, scanned under condition A($\omega/2\theta$) with Ge(Li) detector; (*c*) 18 K, scanned under condition A(ω) with Si(Li) detector; (*d*) 18 K, scanned under condition B(ω) with Si(Li) detector. The reciprocal space geometry appropriate to each scan is illustrated.

3. Results

Bragg Peak Scans

Bragg peak scans about the (440) reflection centred at $\theta = 31°$ were taken for the conditions described above at temperatures of 11, 18, 25 and 293 K. A representative set of the scans is shown in Fig. 2, where each scan shows two sets of measured points, I_θ and I_θ^a, together with the calculated values for the elastic and inelastic contributions to the total scattering. The peak widths depend on the scanning mode as already described by Ti *et al.* (1982). The majority of these scans show the expected single maximum for both the elastic and inelastic components (e.g. Fig. 2*a*) but there are exceptions to this normal situation.

The most interesting exception is seen in the A($\omega/2\theta$) scan taken at 18 K (Fig. 2*b*) for which the total intensity has a rather flat-topped appearance which decomposes into a double-humped elastic peak and a rather sharp and enlarged inelastic peak. There has not been any previous observation of such an elastic peak in Mössbauer scattering experiments. Furthermore, A($\omega/2\theta$) scans made at 11 and 25 K exhibited normal maxima for both I_e and I_i. Some of the scans also showed a small asymmetry in the elastic peak towards lower angles as seen in Fig. 2*c*.

Minima were also observed in the centre of the *inelastic* peaks in the scans A(ω) and B(ω) taken at 25, 18 and possibly at 11 K. The data taken at 18 K, shown in Figs 2*c* and 2*d*, are representative of these peaks. Repeated scans of several of the peaks verified the existence of these minima. Such minima have been observed previously in the inelastic component of γ-ray diffraction peaks for several materials (O'Connor and Butt 1963; Zasimov *et al.* 1976; Kashiwase *et al.* 1982) and have been variously explained in terms of geometrical effects associated with the dynamical scattering (S. W. Wilkins, L. T. Chadderton and T. F. Smith, to be published), rather than as resulting from the intrinsic physical properties of the material concerned.

It is not clear from the present measurements whether the double-peak structure found for the elastic peak in the A($\omega/2\theta$) scan may also be due to geometrical effects, or whether it arises from the inherent physical properties of V_3Si. This question and the nature of the minima in the inelastic peaks are to be examined further with more detailed measurements in a new spectrometer with improved angular resolution.

All the (421) scans showed single symmetrical peaks.

Variable Temperature Data

The data from the variable temperature runs, which were taken under conditions (5)–(8) described in Section 2, are shown in Figs 3–6. These runs were taken as the sample was slowly cooled from room temperature. Each datum point required approximately one hour of counting. All these runs exhibit unusually strong temperature dependences of the total intensity which are associated with peaks near 18 K. By way of comparison, the total intensity for the (400) peak for a single crystal of copper was found to be constant below 75 K.

The intensity measured with the absorber in the scattered beam (I_θ^a) also has a strong temperature dependence which for three of the runs also involved peaks close to 18 K. The separation of the total scattered intensity into its elastic and inelastic components was calculated from the smooth curves which are shown drawn through the I_θ and I_θ^a data points. With the notable exception of the run made in setting A (Fig. 3) the temperature dependence for the elastic intensity follows closely that for the total intensity. A more detailed description of the various features in the elastic and inelastic intensities is given with their interpretations in the next section.

Chronologically, the first measurements as a function of temperature were made in setting A. Several repetitions of the I_θ measurements, including runs using different

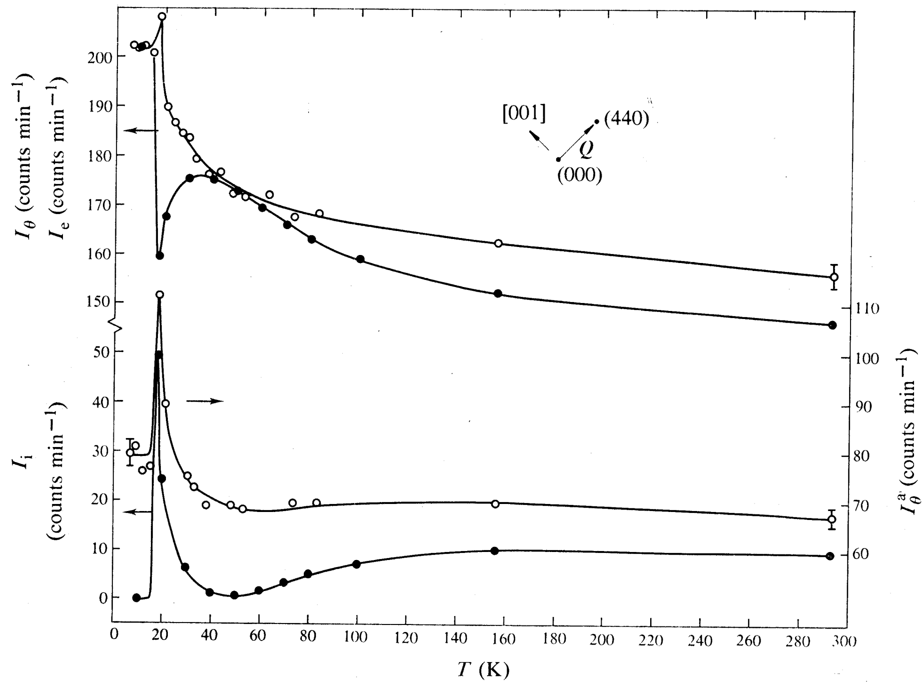

Fig. 3. Variation of I_θ, I_θ^a, I_e and I_i as a function of temperature for the (110) crystal in setting A. Open symbols represent the measured quantities I_θ and I_θ^a; solid symbols are the values of I_e and I_i calculated from the smooth curves drawn through the measured data points.

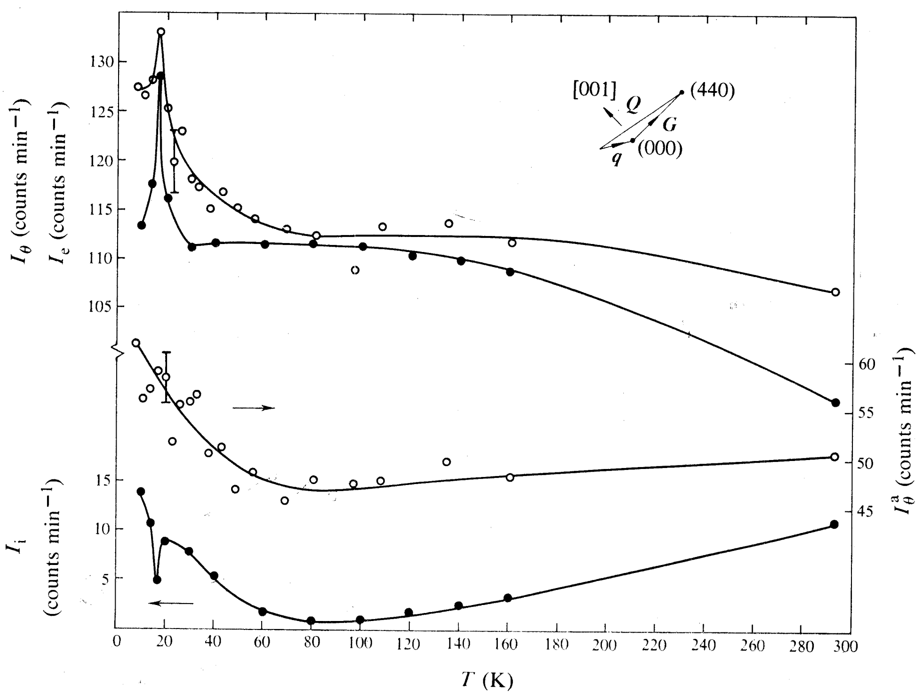

Fig. 4. As for Fig. 3 but under condition A(2θ) such that $|q| \sim 0\cdot13$ Å^{-1}.

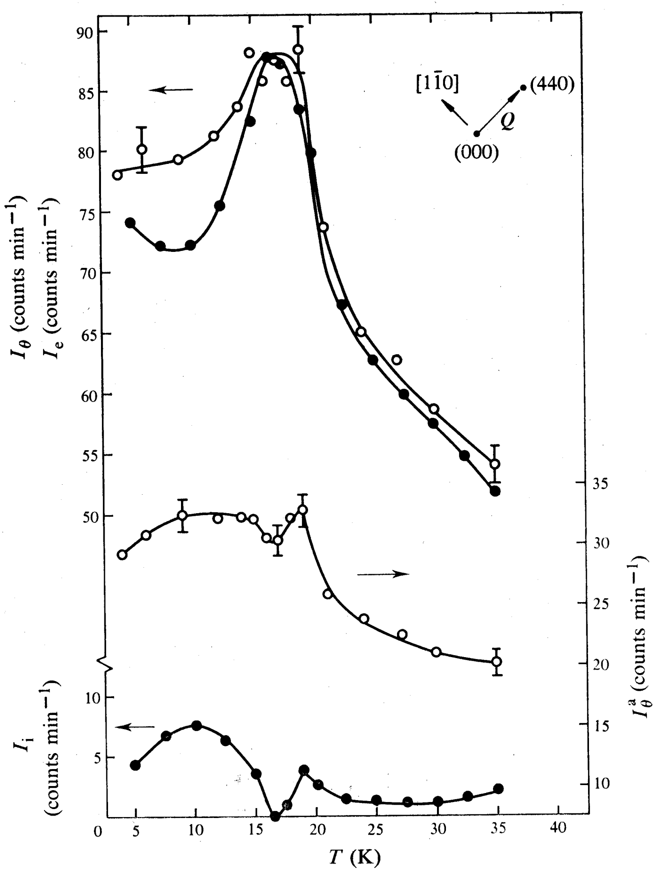

Fig. 5. As for Fig. 3 with the crystal in setting B.

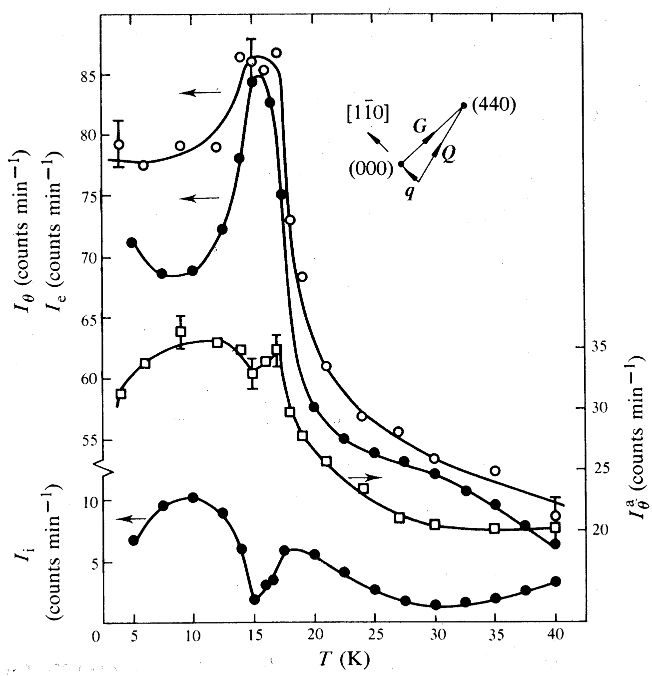

Fig. 6. As for Fig. 3 but under condition B(ω) such that $|q| \sim 0{\cdot}07$ Å^{-1}.

glues to attach the sample to its support, were made to establish the reproducibility of the peak on cooling. A distinct quantitative difference was found between those measurements where the sample was slowly cooled from room temperature and those for slow warming after the sample had been cooled to 4 K as rapidly as the cryostat would allow (approximately one hour). In the latter case there was no evidence of peaks in either I_θ or I_θ^a. However, the presence of a peak in I_θ on warming following a slow cool was established.

In conjunction with one of the cooling runs made in setting A, the signal from the secondary of a pair of coils placed around the sample was monitored as a function of temperature. The sharp drop in scattered intensity was observed to be coincident with the onset of superconductivity.

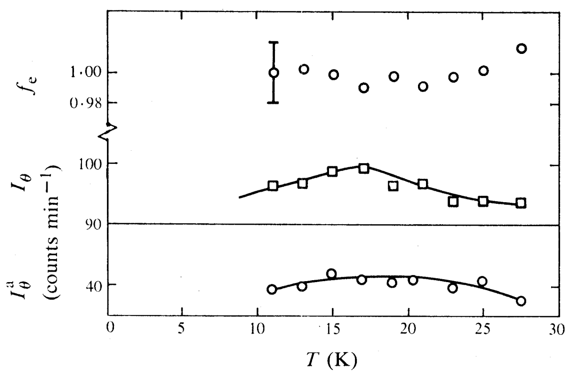

Fig. 7. Variation of I_θ, I_θ^a and the elastic fraction f_e as a function of temperature for the (421) crystal.

The relatively featureless temperature run for the (421) crystal is shown in Fig. 7 and it can be seen to be weakly peaked around 18 K. Decomposition into the elastic and inelastic components shows that this scattering is almost entirely elastic in nature.

4. Discussion

The detailed interpretation of the present scattering data is complicated by the relatively poor k-space resolution. The one-phonon contribution to the inelastically scattered intensity in the vicinity of the reciprocal lattice point defined by the vector $\boldsymbol{G}$ is determined by $\sum_j \boldsymbol{Q}\cdot\boldsymbol{e}_j(\boldsymbol{q})$, where $\boldsymbol{Q}$ is the scattering vector and $\boldsymbol{e}_j(\boldsymbol{q})$ is the polarization unit vector for the jth phonon mode with wave vector $\boldsymbol{q} = \boldsymbol{Q}-\boldsymbol{G}$. As $\boldsymbol{Q}$ is always close to [110] in our measurements, in principle only those phonon modes with $\boldsymbol{e}_j(\boldsymbol{q})$ parallel to [110] should make any significant contribution to the inelastic scattering. Unfortunately, as the volume of k space sampled is relatively large and its shape is unknown, it is impossible to assign the observed scattering to a particular phonon mode unambiguously.

This limitation on the detailed interpretation of the present measurements is illustrated by the marked difference between the temperature dependences for the scattered intensities for the $\boldsymbol{q} = 0$ runs made in settings A and B for the same Bragg reflection (Figs 3 and 5 respectively). While the total intensity for the (440) reflection increases as the temperature decreases and peaks at around 18 K for both orientations of the crystal, the elastic and inelastic components follow dramatically different temperature dependences. For orientation B, the elastic contribution closely follows the same temperature dependence as that for the total scattered intensity and peaks close to 17 K whereas, in orientation A, the elastic contribution decreases below ~ 35 K reaching a minimum value close to 18 K before abruptly increasing. In the latter case, the variation of the inelastic intensity complements that for the elastic intensity, increasing below 40 K and then abruptly dropping below 18 K. In contrast, I_i for orientation B has a considerably weaker temperature dependence, though evidence of a small local minimum around 18 K, superimposed upon a broad maximum, is seen.

The significance of the k-space resolution is emphasized by the marked changes in the temperature dependences of I_e and I_i that result from the relatively small displacement from the Bragg condition, represented by the orientation A(2θ) with $q \sim 0 \cdot 13$ Å^{-1} (Fig. 4). Further evidence of the sensitivity of I_e to both $\boldsymbol{q}$ and temperature is seen in the dip which occurs in the elastic intensity for the A($\omega/2\theta$) scan made at 18 K (Fig. 2*b*), but which was absent in similar scans made at 11 and 25 K.

In general, the major features that are observed in the temperature dependence of I_e and I_i for orientation B are also seen in the measurements made in the off-Bragg conditions A(2θ) and B(ω). We identify these features as:

(1) the strong increase and peaking of I_e as the temperature decreases below ~ 40 K;

(2) the dip in I_i, superimposed upon a broad maximum.

Furthermore, we note that both the peak in I_e and the dip in I_i are centred about the superconducting transition temperature.

In attempting to interpret the above observations it is important to distinguish between elastic and inelastic scattering in the present context. The energy resolution of the absorber sets an upper limit of less than $\pm 4 \times 10^{-8}$ eV on the energy change for a scattering event to be classed as elastic. Thus, apart from the obvious inclusion of those phonons with energies less than this into the elastic scattering, it also implies that lattice fluctuations with lifetimes longer than $\sim 2 \times 10^{-8}$ s will give rise to elastic scattering, whereas for shorter lifetimes the scattering will be inelastic.

The relatively featureless temperature dependence for the intensity of the (421) reflection (Fig. 7) leads us to associate the anomalous temperature dependences of I_e and I_i for the (440) reflection with atomic displacements in the $\{110\}$ planes. Earlier neutron scattering studies on Nb_3Sn (Axe and Shirane 1973) have shown the development of strong elastic central mode ($\boldsymbol{q} = 0$) scattering in addition to the inelastic scattering associated with the soft phonon mode $\boldsymbol{q}$ parallel to [110] and $\boldsymbol{e}$ parallel to [1$\bar{1}$0], as the temperature approaches the critical temperature for the cubic to tetragonal distortion. We note that there is a strong similarity between the temperature dependence for I_e in the present measurements (with the exception of the A run) and that found for the central component in the neutron critical scattering spectrum (Axe and Shirane 1973). Thus, we are led to associate the anomalous increase in I_e with the central mode scattering.

In their discussion of the origin of the central mode scattering, Axe and Shirane (1973) favoured a dynamical model based upon the one-phonon response of the lattice rather than a simple static-strain field model in which atomic displacements result in diffuse (Huang) scattering (Dederichs 1973). From the present results we have no reason to give preference to either of these explanations, though we would note that if the dynamical model is to be applicable then the fluctuations responsible for the central mode are extremely long-lived. It is quite plausible that some temperature-dependent strain field mechanism leading to either a reduction in the static atomic displacements or an increase in their long-range correlation could lead to the observed temperature dependence of I_e. The possibility that a temperature-dependent strain due to residual stress exercises a significant influence on the physical properties of A15 compounds has already been suggested in connection with the thermal expansion (Gibbs *et al.* 1981; Finlayson *et al.* 1981). It is proposed to investigate further the possibility of Huang scattering by a determination of the detailed angular distribution of the scattered intensity about the (440) reflection.

The atomic displacements associated with the cubic to tetragonal distortion for Nb_3Sn involve the pairing of the niobium atoms along two of the linear chain directions [$\Gamma_{12}(+)$ distortion] (Shirane and Axe 1971), so we are further led to infer that in V_3Si it is the dynamics of the vanadium atoms which are responsible for the anomalous temperature dependence of the inelastic scattering. This conclusion is consistent with the development of pronounced anharmonicity in the motion of the vanadium atoms as the temperature is decreased, as proposed by Staudenmann and Testardi (1979). From X-ray intensity measurements made at 300, 78 and 13·5 K they observed an anomalously large increase in the values of the second- and fourth-order atomic displacements, $\langle u^2 \rangle$ and $\langle u^4 \rangle$ respectively, relative to those expected for a harmonic lattice.

Staudenmann and Testardi also reported that reflections for which $(\sin\theta)/\lambda < 0{\cdot}7$ Å^{-1} [which includes the (440) reflection] exhibit an anomalous temperature dependence, which they suggested is due to changes in the real-space electron density distribution with temperature. Staudenmann (1978), in an earlier report, specifically identified such changes with the bond between the Si atoms and the V–V atomic chain, concluding that the distortion from the cubic state occurs when this bond has disappeared. With such a strong connection between lattice stability and electronic configuration, the change in the electronic density of states due to transition to the superconducting state can be expected to have a profound effect upon the lattice dynamics. The arrest of the elastic softening in the superconducting state, as observed by sound-velocity measurements for V_3Si, is well known (Testardi and Bateman 1967). Furthermore, the importance of the electron–phonon interaction in the damping of the [110] transverse phonons in Nb_3Sn and the reduction in damping that occurs below the superconducting transition temperature have been demonstrated by Axe and Shirane (1973).

Within the framework of the present interpretation of the elastic and inelastic scattering it appears that the onset of the superconducting state suppresses both the central mode and the soft mode scattering. The recovery of the latter, as evidenced by the continued large inelastic scattering in the region below T_c, is consistent with a decrease in the soft mode damping as the quasiparticle scattering in the superconducting state decreases.

We propose to investigate further the temperature dependence and anisotropy of the elastic and inelastic Bragg scattering for transforming and non-transforming crystals of V_3Si using a spectrometer with improved angular resolution.

Acknowledgments

We have benefited from discussions with a number of colleagues during this work and we would like to thank in particular L. T. Chadderton, S. L. Mair, S. W. Wilkins,

T. J. Hicks and P. Lloyd. The financial support of the Monash University Special Research Fund and the Australian Research Grants Scheme are gratefully acknowledged.

References

Albanese, G., and Ghezzi, C. (1972). *Phys. Rev.* B **5**, 1746.
Axe, J. D., and Shirane, G. (1973). *Phys. Rev.* B **8**, 1965.
Dederichs, D. D. (1973). *J. Phys.* F **3**, 471.
Finlayson, T. R., Gibbs, E. E., and Smith, T. F. (1981). *Physica* B & C **107**, 1011.
Gibbs, E. E., Finlayson, T. R., and Smith, T. F. (1981). *Solid State Commun.* **37**, 33.
Kashiwase, Y., Kainuma, Y., and Minoura, M. (1982). *J. Phys. Soc. Jpn* **51**, 937.
Kodess, B. M. (1974). *Sov. Phys. Solid State* **16**, 782.
Mathieson, A. McL. (1982). *Acta Crystallogr.* A **38**, 378.
O'Connor, D. A. (1972). *In* 'Perspectives in Mössbauer Spectroscopy' (Eds S. G. Cohen and M. Pasternak), p. 171 (Plenum: New York).
O'Connor, D. A., and Butt, N. M. (1963). *Phys. Lett.* **7**, 233.
Shirane, G., and Axe, J. D. (1971). *Phys. Rev.* B **4**, 2957.
Shirane, G., Axe, J. D., and Birgeneau, R. J. (1971). *Solid State Commun.* **9**, 397.
Smith, T. F. (1972). *J. Low Temp. Phys.* **6**, 461.
Staudenmann, J.-L. (1978). *Solid State Commun.* **26**, 461.
Staudenmann, J.-L., and Testardi, L. R. (1979). *Phys. Rev. Lett.* **43**, 40.
Testardi, L. R. (1973). *In* 'Physical Acoustics', Vol. 10 (Eds W. P. Mason and R. N. Thurston), p. 193 (Academic: London).
Testardi, L. R., and Bateman, T. B. (1967). *Phys. Rev.* **154**, 402.
Ti, S. S., Clark, P. E., and Cashion, J. D. (1982). *Nucl. Instrum. Methods* **203**, 533.
Viswanathan, R., and Johnston, D. C. (1976). *Phys. Rev.* B **13**, 2877.
Viswanathan, R., and Luo, H. H. (1971). *Solid State Commun.* **9**, 1733.
Zasimov, V. S., Lobanov, N. N., Rüdiger, J., and Kusmen, R. M. (1976). *Phys. Status Solidi* (*a*) **38**, K45.

Manuscript received 9 September 1982, accepted 18 January 1983